Liquid Crystals
Publication details, including instructions for authors and subscription information:
http://www.informaworld.com/smpp/title~content=t713926090

Dispersion relations for liquid crystals using the anisotropic Lorentz model with geometrical effects

I. Abdulhalim[a]
[a] Department of Electrooptics Engineering, Ben Gurion University, Beer Sheva 84105, Israel

To cite this Article Abdulhalim, I.(2006) 'Dispersion relations for liquid crystals using the anisotropic Lorentz model with geometrical effects', Liquid Crystals, 33: 9, 1027 — 1041
To link to this Article: DOI: 10.1080/02678290600804896
URL: http://dx.doi.org/10.1080/02678290600804896

Liquid Crystals, Vol. 33, No. 9, September 2006, 1027–1041

Dispersion relations for liquid crystals using the anisotropic Lorentz model with geometrical effects

I. ABDULHALIM

Department of Electrooptics Engineering, Ben Gurion University, P.O. Box 653, Beer Sheva 84105, Israel; e-mail: abdulhlm@bgu.ac.il

(*Received 24 February 2006; accepted 5 April 2006*)

The dispersion relations for the refraction indices and extinction coefficients of an ordered system of anisotropic molecules are derived, taking into account absorption near the resonance frequencies and the molecular geometrical form factor. The derivation is based on a combination of the anisotropic Lorentz oscillator dispersion model and the generalized Lorentz–Lorentz (LL) relationship. This relationship is shown to be consistent with the isotropic limit. The geometrical form tensor (GFT) distinguishes this relationship from the LL and the Calusius–Mossotti equations valid for isotropic media. Far from the absorption bands the dispersion relationships are shown to converge to those of Sellmeier-type dispersion relationships for transparent dielectrics that can be expanded into generalized Cauchy-type series. The principal values of the GFT are shown to cause a red shift to the resonance wavelengths that can be found from measurements in the disordered phase. Experimental data are presented based on published works as well as measurements using a spectroscopic retardation technique, and excellent agreement is obtained with the theoretical calculations on several LC materials.

1. Introduction

Linear and nonlinear optical properties of liquid crystals (LCs) are a subject of growing interest, because of their strong electro-optic effects useful for a variety of applications as well as for the study of their physical phenomena [1]. Therefore it is of great importance to have accurate dispersion dependences of their refractive indices. Such relationships have been derived in the past by several investigators [2–9] and used for fitting to the experimental data [2, 9–12]. The derivation of the dispersion relationship relies strongly on the relation between the polarizability tensor and the dielectric tensor. Such relationships have to take into account the anisotropy of the constituent particles and their geometrical form as well as the damping factor of the absorption resonance peaks, in particular in the visible range of the spectrum, which is not far enough from the UV electronic absorption. Attempts to generalize the Lorentz–Lorentz (LL) or the Calusius–Mossotti (CM) equations to crystals taking into account the geometrical form tensor (GFT) in the depolarization fields existed since the first half of the 19th century [13–15], and some were considered for application to liquid crystals [16–22] in particular to explain the temperature dependence of their polarizability [22–25]. Neugebauer [14] obtained an equation similar to the LL equation:

$$\frac{\varepsilon_q - 1}{\varepsilon_q + 2} = \frac{4\pi N}{3}\beta_q \tag{1}$$

where the parameter β_q was called the apparent polarizability and ε_q with $q=1, 2, 3$ being the principal values of the dielectric tensor. Although Neugebauer took the crystal shape into account, he did not consider the anisotropic geometrical shape of the molecules or constituent particles. Saupe and Maier [16] have modified the Neugebauer relationship and obtained the following formulae:

$$\varepsilon_q - 1 = 4\pi N H_q \alpha_q \tag{2}$$

where $H_q=(1-NL_q\alpha_q)^{-1}$ are called the local field factors and L_q are the internal field constants; N is the number density of molecules and α_q the corresponding principal values of the polarizability tensor. Equation (2) may then be designated as the Neugebauer–Saupe–Maier or simply NSM relationship. Although equation (2) is in fact the most accurate within the mean field theory, it did not become popular because it did not show a good fit with experimental data. In an attempt to improve the fit between measured and calculated data for several molecular crystals, Vuks [15] derived a slightly modified form of equation (1).

Liquid Crystals
ISSN 0267-8292 print/ISSN 1366-5855 online © 2006 Taylor & Francis
http://www.tandf.co.uk/journals
DOI: 10.1080/02678290600804896

Vuks's equation is written as:

$$\frac{\varepsilon_q - 1}{\langle\varepsilon\rangle + 2} = \frac{4\pi N}{3}\alpha_q \tag{3}$$

where <ε> is the average of the principal values of the dielectric tensor. The difference between Vuks's relationship and the LL or CM equations is that in the denominator the average value is replaced by the principal value itself, that is: $<\varepsilon>\leftrightarrow\varepsilon_q$. In the derivation of Vuks's equation the following linear relationship between the local and macroscopic fields was used:

$$E = \frac{\langle\varepsilon\rangle + 2}{3}E_0. \tag{4}$$

This is a crude approximation because it ignores the geometrical shape of the molecules and simply uses the equivalent to the isotropic case with the dielectric constant replaced by the average <ε>. An additional apparent problem with Vuks's relation is the coupling it introduces between the principal values ε_q via the averaged dielectric constant in the left hand side of equation (3). In the limit of a perfectly ordered system there is no justification for this coupling. De Jeu *et al.* [19, 20] questioned the validity of Vuks's equation and made additional progress based on the Neugebauer model by taking into account the geometrical shape of the molecules and applying the statistical average over the LC molecular orientations. In their approach, however, they performed the average over the dielectric tensor rather than the polarizability. This caused inconsistency between their expression and the CM or LL equations, as can be seen from the fact that it does not converge to them in the isotropic limit. A modification to the de Jeu *et al.*, model was performed by Ibrahim and Hass [21] who introduced an additional tensor relating the macroscopic field to the cavity field; however their final expression did not remove the inconsistency with the isotropic case. Chandrasekhar and Madhusudana [17] proposed a relationship that basically uses the LL equation with the average values for the polarizability and dielectric tensor:

$$\left(1 - \frac{4}{3}\pi N\langle\alpha\rangle\right)^{-1} = \frac{\langle\varepsilon\rangle + 2}{3}. \tag{5}$$

Pelzl [18] on the other hand used the LL equation without taking into account the geometrical form factors:

$$\left(1 - \frac{4}{3}\pi N\alpha_q\right)^{-1} = \frac{\varepsilon_q + 2}{3}. \tag{6}$$

Lately Kedzierski *et al.* [25] have critically studied the temperature dependence of the polarizability tensor and the local field anisotropy factors and made comparative study of the relationships (1)–(6). Surprisingly they found that Vuks's relationship better fits the experimental data, while when using the NSM relationship they had to incorporate only very small anisotropy to the geometrical form factors. In order to find the dispersion dependence for the birefringence, Wu and coworkers [3, 5, 7, 9] derived an approximate expression based on Vuks's relationship and the following quantum mechanical expression for the polarizability:

$$\alpha_{\parallel,\perp}(\lambda) = g_{\parallel,\perp}\frac{\lambda^2\lambda^{*2}}{\lambda^2 - \lambda^{*2}} \tag{7}$$

where λ^* is the wavelength of the nearest absorption band and $g_{\parallel,\perp}$ are the oscillator strengths parallel and perpendicular to the molecular axis. They obtained a good fit with the experimental data [7, 9]. Later, the present author [6] derived exact and explicit forms for the dispersion relationships of the refractive indices based on Vuks's relationship and used them for calculating the effective refractive indices of ferroelectric liquid crystals and their electro-optic response [26–28]. The derived expressions based on Vuks's relationship can be written as [6]:

$$\varepsilon_\perp = \frac{1 + a(7\alpha_\perp - \alpha_\parallel)}{1 - a(2\alpha_\perp + \alpha_\parallel)} \tag{8 a}$$

$$\varepsilon_\parallel = \frac{1 + 2a(4\alpha_\parallel - \alpha_\perp)}{1 - a(2\alpha_\perp + \alpha_\parallel)} \tag{8 b}$$

and in the single band approximation one obtains [6]:

$$n_{\parallel,\perp} = \left(\frac{G_{\parallel,\perp}\lambda^2 - 1}{G_c\lambda^2 - 1}\right)^{\frac{1}{2}} \tag{8 c}$$

where $G_\perp = \lambda^{*-2} + a(7g_\perp - g_\parallel)$, $G_\parallel = \lambda^{*-2} + 2a(4g_\parallel - g_\perp)$, and $G_c = \lambda^{*-2} - a(2g_\perp + g_\parallel)$ with $a = 4\pi N/9$. As can be seen from these expressions, the indices $n_{\perp,\parallel}$ are both determined by coupled parameters $G_{\perp,\parallel}$ and G_c, which has no justification in a perfectly ordered system. The expressions derived by Lam *et al.* [4], using the *ab initio* calculation based on a three body model can also be written in a similar form to equation (8 *c*), however the G_c constant in their formulation has two different values for $n_\perp$ and $n_\parallel$, simply because two different spring constants are assumed along the two directions ∥ and ⊥; that is, $\lambda^*_\parallel \neq \lambda^*_\perp$. In fact the relations of Lam *et al.* have the same form obtainable when equation (7) is used in the Neugebauer relationship (1).

Equations (8), and variations of them using power series expansion and more than one absorption band,

have been used extensively in the liquid crystals literature [3, 5, 7, 9]. The fits to experimental data are satisfactory in most cases, however more than one absorption band was needed in certain other cases. The motivation for this article is to present dispersion relationships that take into account the form birefringence and dissipation effects, so that dispersion relationships for the extinction coefficients are also obtained. In the next section a formulation is presented for the optical response of anisotropic oscillators within the Lorentz model. In § 3 this formulation is applied to liquid crystals. In § 4 some simplified forms are presented for dispersion relationships useful for fit to experimental data. In § 5 a comparison with existing experimental data is presented and discussed, and in § 6 experimental results are presented for several LC materials with a theoretical fit based on the proposed formulation.

2. Response of anisotropic Lorentz oscillators

Our starting point is a model for an anisotropic molecule that is considered as a collection of dipoles induced by an external electromagnetic field having wavelength λ and frequency $\omega = 2\pi c/\lambda$. In 3D space the oscillating charges along the x, y and z axes in orthogonal coordinate system gain potential energy represented by the interaction potential:

$$U = \frac{1}{2}\sum_i \sum_j K_{ij} u_i u_j \tag{9}$$

where $i, j = x, y, z$ and $u_{i,j}$ are the displacements of the oscillating masses along x, y or z, from the equilibrium positions. The matrix K_{ij} is the 2nd rank tensor of spring constants, which is symmetric. In the principal axis system with orthonormal basis vectors $\hat{\mathbf{e}}_1, \hat{\mathbf{e}}_2, \hat{\mathbf{e}}_3$, this tensor becomes diagonal $K_{pq} = \delta_{pq} K_{qq}$ where δ_{pq} is the Kronecker delta function and $p,q = 1, 2, 3$. Assuming effective masses m_1, m_2, m_3 oscillating along the three principal axes with corresponding frequencies ω_1, ω_2, ω_3, the diagonal spring constants tensor is given by:

$$K_{pq} = \delta_{pq} m_q \omega_q^2. \tag{10}$$

The displacement vector $\mathbf{u} = \{u_x, u_y, u_z\}$ is transformed to the principal axis system through a rotation transformation R such that: $\mathbf{u}' = \{u_q\} = R\mathbf{u}$ where $q = 1, 2, 3$. For a monochromatic harmonic EM field acting on the dipoles in the principal axis system, we have $\mathbf{E}_0 = \mathbf{E}_0(\omega)\exp(-i\omega t)$, with $\mathbf{E}_0(\omega) = \{E_{01}, E_{02}, E_{03}\}$. Assuming the local field amplitudes given by: $\mathbf{E}(\omega) = \{E_1, E_2, E_3\}$, the equations of motion of the oscillating masses become:

$$m_q \frac{\mathrm{d}^2 u_q}{\mathrm{d}t^2} = Q_q E_q - \gamma_q \frac{\mathrm{d}u_q}{\mathrm{d}t} - \sum_q K_{pq} u_q \tag{11}$$

where Q_q with $q = 1, 2, 3$, is the effective oscillating charge and γ_q is the corresponding damping constant. Inserting the harmonic solution: $\mathbf{u}' = \{u_q(\omega)\}\exp(-i\omega t)$ into equation (11) we find the following solution:

$$\{u_q(\omega)\} = \left[K_{pq} - \left(m_q\omega^2 + i\gamma_q\omega\right)\boldsymbol{I}_{3\times 3}\right]^{-1}\{Q_q\}\mathbf{E}(\omega) \tag{12}$$

where $\boldsymbol{I}_{3\times 3}$ is a 3×3 unit matrix. The molecular dipole polarization vector is therefore:

$$\begin{aligned} p_q(\omega) &= \{Q_q u_q(\omega)\} \\ &= \left[K_{pq} - \left(m_q\omega^2 + i\gamma_q\omega\right)\boldsymbol{I}_{3\times 3}\right]^{-1}\left\{Q_q^2\right\}\mathbf{E}(\omega) \end{aligned} \tag{13}$$

and by definition, the linear molecular polarizability tensor is:

$$\alpha_{pq}(\omega) = \left[K_{pq} - \left(m_q\omega^2 + i\gamma_q\omega\right)\boldsymbol{I}_{3\times 3}\right]^{-1}\left\{Q_q^2\right\} \tag{14}$$

which is a diagonal matrix with the following components:

$$\alpha_{qq}(\omega) = \frac{Q_q^2}{m_q\left(\omega_q^2 - \omega^2 - i\gamma_q\omega/m_q\right)}. \tag{15}$$

In quantum theory this expression becomes:

$$\alpha_{qq}(\omega) = \sum_l \frac{f_{qkl}^*}{\left(\omega_{qkl}^2 - \omega^2 - i\Gamma_q\omega\right)} \tag{16}$$

where ω_{qkl} is the frequency of the electric dipole transition between the two quantum states k and l along the principal axis direction q, with f_{qkl}^* being the effective oscillator strength and Γ_q the corresponding damping constant.

3. Application to liquid crystals

Since most of the liquid crystals are uniaxial we restrict the calculation now to this case, although the generalization to the biaxial case is straightforward. For uniaxial media the two principal values of the molecular polarizability are:

$$\alpha_{\parallel,\perp}(\omega) = \sum_l \frac{f_{\parallel,\perp kl}^*}{\left(\omega_{\parallel,\perp kl}^2 - \omega^2 - i\Gamma_{\parallel,\perp}\omega\right)} \tag{17}$$

where the subscripts $\parallel$ and $\perp$ designate directions parallel and perpendicular to the molecular long axis, respectively. For a uniaxial liquid crystal the statistical averaging over the director orientations leads to the

following expression for the macroscopic polarizabilities, following Maier and Saupe [29]:

$$\langle\alpha\rangle_{\mathrm{e}}=\frac{1}{3}\left[(1+2S)\alpha_{\parallel}+2(1-S)\alpha_{\perp}\right] \tag{18}$$

$$\langle\alpha\rangle_{\mathrm{o}}=\frac{1}{3}\left[(1-S)\alpha_{\parallel}+(2+S)\alpha_{\perp}\right]. \tag{19}$$

Where S is the order parameter, such that for a perfect crystal $S=1$ and we get $<\alpha>_{\mathrm{e,o}}=\alpha_{\parallel,\perp}$; while for an isotropic liquid $S=0$ and we get the average polarizability $<\alpha>_{\mathrm{e,o}}=(\alpha_{\parallel}+2\alpha_{\perp})/3=\alpha_{\mathrm{av}}$. The local field $\mathbf{E}$ is related to the macroscopic field $\mathbf{E}_0$ by:

$$\mathbf{E}=\mathbf{E}_0+\widetilde{\mathbf{L}}.\mathbf{P} \tag{20}$$

where $\widetilde{\mathbf{L}}$ is a 2nd rank tensor known as the geometrical form tensor (GTF) or Lorentz tensor [13, 30–33], which takes into account the shape of the molecules. This tensor is the key in explaining the form birefringence of anisotropic molecules and other ordered systems composed of asymmetric entities. For a spherical molecule the principal values of this tensor become equal to $4\pi/3$, while for other spheroids the general expressions are given in the appendix. The relationship between the polarization vector and the macroscopic field is:

$$\mathbf{P}=\frac{1}{4\pi}(\widetilde{\boldsymbol{\varepsilon}}-\boldsymbol{I}_{3\times 3})\mathbf{E}_0 \tag{21}$$

where $\boldsymbol{\varepsilon}$ is the dielectric tensor. In addition, the polarization and the local field are related by:

$$\mathbf{P}=N\widetilde{\alpha}\mathbf{E}. \tag{22}$$

Using equations (20)–(22) we get:

$$\widetilde{\boldsymbol{\varepsilon}}=\boldsymbol{I}_{3\times 3}+\frac{4\pi N\widetilde{\alpha}}{1-N\widetilde{\alpha}\widetilde{\mathbf{L}}} \tag{23}$$

The principal values of the dielectric tensor for the uniaxial case are then given by:

$$\varepsilon_{\mathrm{e,o}}=1+\frac{4\pi N\langle\alpha\rangle_{\mathrm{e,o}}}{1-N\langle\alpha\rangle_{\mathrm{e,o}}L_{\mathrm{e,o}}} \tag{24}$$

where for the LC medium with a certain degree of order S, the form factors $L_{\mathrm{e,o}}$ are related to the molecular form factors $L_{\parallel,\perp}$ by relationships similar to equations (18) and (19) and the normalization condition (see appendix) $L_{\mathrm{e}}+2L_{\mathrm{o}}=4\pi$, applies. For a prolate spheroid $L_{\parallel}<L_{\perp}$, so that L_{e} and L_{o} behaviour with the order parameter is opposite to the behavior of α_{e} and α_{o}, following equations (18) and (19). Note that, based on equation (24) the two principal refractive indices are determined by coupled parameters only due to the averaging over the molecular orientations when the order parameter $S<1$; while for a perfectly ordered system with $S=1$ the coupling between these parameters disappears as expected. It should also be noted that this expression coincides with the CM equation. For an isotropic medium: $S=0$, $<\alpha>_{\mathrm{e,o}}=(\alpha_{\parallel}+2\alpha_{\perp})/3=\alpha_{\mathrm{av}}$, $L_{\mathrm{e,o}}=4\pi/3$ and the result is:

$$\varepsilon_{\mathrm{iso}}=1+\frac{4\pi N\alpha_{\mathrm{av}}}{1-\frac{4\pi}{3}N\alpha_{\mathrm{av}}}. \tag{25}$$

The reason for the inconsistency of the de Jeu *et al.* expression with the CM equation is because in their calculation the statistical average over the dielectric tensor was taken. In our case averaging over the polarizability tensor was taken, which makes more sense since the polarizability has a more microscopic meaning than has the dielectric tensor. For comparison purposes with the Vuks and LL relationships we write equation (24) in the following form:

$$\frac{\varepsilon_{\mathrm{e,o}}-1}{\varepsilon_{\mathrm{e,o}}+(4\pi/L_{\mathrm{e,o}}-1)}\frac{4\pi}{3L_{\mathrm{e,o}}}=\frac{4\pi N}{3}\langle\alpha\rangle_{\mathrm{e,o}}. \tag{26}$$

For the general biaxial case this may be written as:

$$\frac{\varepsilon_{\mathrm{q}}-1}{\varepsilon_{\mathrm{q}}+\left(4\pi/\langle L\rangle_q-1\right)}=\langle L\rangle_q N\langle\alpha\rangle_q \tag{27}$$

where $q=1, 2, 3$. This relation represents a modified LL relationship applicable to anisotropic media and reduces to the isotropic case when $L_q=4\pi/3$.

4. Simplified dispersion relationships

In terms of the wavelength, each absorption band contributes the following real and imaginary parts of the principal values of the polarizability tensor:

$$\alpha_{q\mathrm{r}}(\lambda)=\frac{g_q\lambda_q^2\lambda^2\left(\lambda^2-\lambda_q^2\right)}{\left(\lambda^2-\lambda_q^2\right)^2+\Lambda_q\lambda_q^4\lambda^2} \tag{28}$$

$$\alpha_{q\mathrm{i}}(\lambda)=\frac{g_q\lambda_q^4\Lambda_q^{\frac{1}{2}}\lambda^3}{\left(\lambda^2-\lambda_q^2\right)^2+\Lambda_q\lambda_q^4\lambda^2} \tag{29}$$

where $g_q=f_q^*\Big/(2\pi c)^2$, and $\Lambda_q=\Gamma_q^2\Big/(2\pi c)^2$. Note that without absorption the imaginary part vanishes since then $\Lambda_q=0$ and equation (28) reduces to the well known expression far from the absorption band, see equation (7). For multiple absorption bands these equations become:

$$\alpha_{q\mathrm{r}}(\lambda)=\sum_j\frac{g_{qj}\lambda_{qj}^2\lambda^2\left(\lambda^2-\lambda_{qj}^2\right)}{\left(\lambda^2-\lambda_{qj}^2\right)^2+\Lambda_{qj}\lambda_{qj}^4\lambda^2} \tag{30}$$

$$\alpha_{qi}(\lambda)=\sum_j \frac{g_{qj}\lambda_{qj}^4\Lambda_{qj}^{\frac{1}{2}}\lambda^3}{\left(\lambda^2-\lambda_{qj}^2\right)^2+\Lambda_{qj}\lambda_{qj}^4\lambda^2}. \tag{31}$$

The corresponding real and imaginary parts of the principal dielectric constants are given by:

$$\varepsilon_{qr}(\lambda)=1+\frac{4\pi\left[\alpha'_{qr}-L'_q\left(\alpha'^2_{qr}+\alpha'^2_{qi}\right)\right]}{\left(1-L'_q\alpha'_{qr}\right)^2+L'^2_q\alpha'^2_{qi}} \tag{32}$$

$$\varepsilon_{qi}(\lambda)=\frac{4\pi\alpha'_{qi}}{\left(1-L'_q\alpha'_{qr}\right)^2+L'^2_q\alpha'^2_{qi}} \tag{33}$$

where we made the replacements $N<\alpha>_{qr,qi}\rightarrow\alpha'_{qr,qi}$ and $<L>_q\rightarrow L'_q$. The refractive index and extinction coefficient are then found from the relationships: $\varepsilon_{qr}=n_q^2-\kappa_q^2$ and $\varepsilon_{qi}=2n_q\kappa_q$. Far from the absorption bands and using the 1st order series approximation $\varepsilon_{qr}(\lambda)\approx 1+4\pi\alpha'_{qr}$ one arrives at a dispersion relationship similar to that of Sellmeir [34] for transparent dielectrics. As we can see, this latest approximation ignores the depolarization and one may use the 2nd order expansion: $\varepsilon_{qr}(\lambda)\approx 1+4\pi\alpha'_{qr}+4\pi L'_q\alpha'^2_{qr}$ and obtain a form of generalized Sellmeir dispersion relationship. It should be noted that one cannot arrive at these results if Vuks's relationship is used.

For the case of no damping, equation (32) yields:

$$n_q=\left[\frac{1+\left(4\pi-L'_q\right)\alpha'_{qr}}{1-L'_q\alpha'_{qr}}\right]^{\frac{1}{2}}. \tag{34}$$

This relationship is very useful, as it will be shown later that damping effects are negligible in the visible range of the spectrum in many cases. Since $\alpha'_{qr}<1$ in particular far away from the absorption resonance, equation (34) can be expanded into a power series, and up to the 5th order we get:

$$n_q\approx 1+a_1\alpha'_{qr}+a_2\alpha'^2_{qr}+a_3\alpha'^3_{qr}+a_4\alpha'^4_{qr}+a_5\alpha'^5_{qr} \tag{35}$$

where:

$$a_1=2\pi;\ a_2=2\pi\left(L'_q-\pi\right);\ a_3=2\pi\left(L'^2_q-2\pi L'_q+2\pi^2\right);$$

$$a_4=2\pi\left(L'^3_q-3\pi L'^2_q+6\pi^2L'_q-5\pi^3\right);$$

$$a_5=2\pi\left(L'^4_q-4\pi L'^3_q+12\pi^2L'^2_q-20\pi^3L'_q+14\pi^4\right).$$

Note that in the absence of absorption the form factor enters only in the non-linear terms. The non-linear terms also reveal non-linear dependence of the refractive indices and the birefringence on the order parameter S. This non-linear dependence was reported recently in particular far from the transition temperatures [35]. From equation (34) we can also write a dispersion relationship equivalent to equation (8) for the single absorption band case and when $S=1$ as follows:

$$n_q=\left(\frac{F_q\lambda^2-1}{F'_q\lambda^2-1}\right)^{\frac{1}{2}} \tag{36}$$

where now $F_q=\lambda_q^{-2}+Ng_q\left(4\pi-L_q\right)$, and $F'_q=\lambda_q^{-2}-Ng_qL_q$. These expressions have the same form as that derived by Lam *et al.* [4], however their expressions for F_q and F'_q are different because they do not take into account the anisotropy of the depolarization form factor L_q.

Series expansion of equation (36) in powers of $1/\lambda$ yields the following Cauchy-type dispersion relation:

$$n_q\approx C_0+\frac{C_2}{\lambda^2}+\frac{C_4}{\lambda^4}+\frac{C_6}{\lambda^6} \tag{37}$$

where

$$C_0=\left(\frac{F_q}{F'_q}\right)^{\frac{1}{2}};\ C_2=\frac{\left(F_q-F'_q\right)}{2F_q^{1/2}F_q'^{3/2}};$$

$$C_4=\frac{\left(F_q-F'_q\right)\left(3F_q+F'_q\right)}{8F_q^{3/2}F_q'^{5/2}};$$

$$C_6=\frac{\left(F_q-F'_q\right)\left(5F_q^2+2F_qF'_q+F'^2_q\right)}{16F_q^{5/2}F_q'^{7/2}}.$$

For the fit to the experimental data to be physical, the fitting parameters should be F_q and F'_q rather than the polynomial coefficients which are determined by F_q and F'_q. In the limit of $\lambda\ll\lambda_q$, we get: $n_{q0}\approx\left(F_q\big/F'_q\right)^{\frac{1}{2}}$, which can be further expanded as:

$$n_{q0}\approx\left(1+\frac{4\pi N\lambda_q^2g_q}{1-N\lambda_q^2g_qL_q}\right)^{\frac{1}{2}}\approx 1+2\pi Ng_q\lambda_q^2+2\pi N^2g_q^2\lambda_q^4L_q. \tag{38}$$

From this equation we can see how the value of the geometrical form factor can affect the resonance frequency. In order to get the same n_{q0} for different values of L_q, the resonance wavelength has to be shifted from its value in the disordered phase by a value given

by:

$$\Delta\lambda_q \approx \frac{Ng_q\lambda_q^3\left(L_q-4\pi/3\right)}{2-Ng_q\lambda_q^2\left(L_q-4\pi/3\right)}. \quad (39)$$

This is an approximate expression, valid when only a single band is considered, however it gives an analytic qualitative behaviour of the dependence of the resonance wavelength shift on the variety of parameters. The strongest effect on the resonance wavelength shift is the parameter g_q; as we shall see later this shift is about 15 nm for the $\sigma\rightarrow\sigma^*$ transition peak located at around 120 nm, while it is less than 2 nm for the $\pi\rightarrow\pi^*$ transitions because their g_q parameters are smaller by at least an order of magnitude.

Ignoring the difference in the resonance wavelengths, that is $\lambda_{\parallel}\approx\lambda_{\perp}$, the birefringence $\Delta n=n_e-n_o$ in this limit maybe written as:

$$\Delta n_0 \approx 2\pi N\lambda_q^2\Delta g_q + 2\pi N^2\lambda_q^4\left(g_e^2L_e - g_o^2L_o\right). \quad (40)$$

This again shows that the birefringence is not a linear function of the order parameter as found lately [36]. Hence the anisotropy in the form factor adds some non-linearity to the birefringence behaviour in relation to the order parameter.

5. Comparison with experimental data

For comparison with experimental data we use available data for the widely studied liquid crystal 5CB, and the Merck materials E7 and E44, using experimental data measured by the spectroscopic retardation technique. The dispersion of LC refractive indices in the visible and the near infrared originates from electronic absorption bands in the UV. These bands are characteristic of the allowed transitions in phenyl rings (benzene). Hence knowledge of the characteristics of the UV absorption spectra is crucial in obtaining a physical fit to the experimental data. The LC 5CB (4-cyano-4′-*n*-pentylbiphenyl) is known to exhibit three electronic absorption bands in the UV at wavelengths: $\lambda_1\approx120$ nm, $\lambda_2\approx200$ nm, $\lambda_3\approx282$ nm. The first band has never been measured experimentally while the last two were reported by Wu *et al.* [3, 5, 7, 9] using polarized UV spectroscopy. The 2nd peak is actually has an additional companion peak at around 214 nm. The measured absorption peak wavelengths are slightly different from those predicted by the molecule symmetry group, due to the effects of long range order in the LC medium represented by the order parameter S, the depolarization field represented by the form factors L_e, L_o and the existence of conjugated π-bonds in the phenyl ring. Tables 1 and 2 summarize the absorption peak wavelengths, oscillator strengths and damping factors used in the fitting to the experimental data. The molecular mass for 5CB is $M=249.359\,\mathrm{g\,mol^{-1}}$, and using a value of $1\,\mathrm{g\,cc^{-1}}$ for the density we obtain the get number density of molecules $N\approx2.415\,\mathrm{nm^{-3}}$.

In figure 1 we show the dispersion curves calculated using equations (30)–(33) and fitted to Li and Wu [9] experimental data in the spectral range 380–820 nm. The experimental data of [9] was approximated using their 3-band model fit. We used an order parameter $S=0.61629$, the same as used in [9], and the fitting parameters are: the absorption peaks parameters summarized in table 1, and the geometrical form factor L_e. The fit is found to be highly sensitive to L_e, giving for the best fit the value: $L_e=4\pi/3.7$; and from the normalization condition we get $L_o\approx4\pi/2.7407$. The ratio $L_e/L_o=0.741$, is not far from the value of

Table 1. Fitting parameters used for the o-wave. The units of the g parameters have dimensions $\mathrm{nm^3}$ while those of the Λ parameters are $\mathrm{nm^2}$. The fitting was made to the experimental data, within the range 370–900 nm.

LC	λ_{1o}	$\Lambda_{1o}\times10^{-7}$	$g_{1o}\times10^{-7}$	λ_{2o}	$\Lambda_{2o}\times10^{-7}$	$g_{2o}\times10^{-9}$	λ_{3o}	$\Lambda_{3o}\times10^{-7}$	$g_{3o}\times10^{-9}$	λ_{4o}	$\Lambda_{4o}\times10^{-7}$	$g_{4o}\times10^{-9}$
5CB	104	7	23.4	195	12	18	215	0.45	8.6	280	0.012	0.0097
E7	104	0.2	22.8	195	12	16	223	0.35	9.8	248	0.086	20
E44	104	0.02	24	195	0.12	16	223	0.15	12	248	0.13	11

Table 2. Fitting parameters used for the e-wave. The units of the g parameters have dimensions $\mathrm{nm^3}$ while those of the Λ parameters are $\mathrm{nm^2}$. The fitting was made to the experimental data, within the range 370–900 nm.

LC	λ_{1e}	$\Lambda_{1e}\times10^{-7}$	$g_{1e}\times10^{-7}$	λ_{2e}	$\Lambda_{2e}\times10^{-7}$	$g_{2e}\times10^{-9}$	λ_{3e}	$\Lambda_{3e}\times10^{-7}$	$g_{3e}\times10^{-9}$	λ_{4e}	$\Lambda_{4e}\times10^{-7}$	$g_{4e}\times10^{-9}$
5CB	122	1.2	24.3	196	1.01	82	216	0.82	10.5	280	0.342	53
E7	122	0.15	23.4	196	0.33	76	223	0.22	11	246	0.087	49
E44	122	0.011	20.1	196	0.055	95	223	0.22	22	246	0.16	110

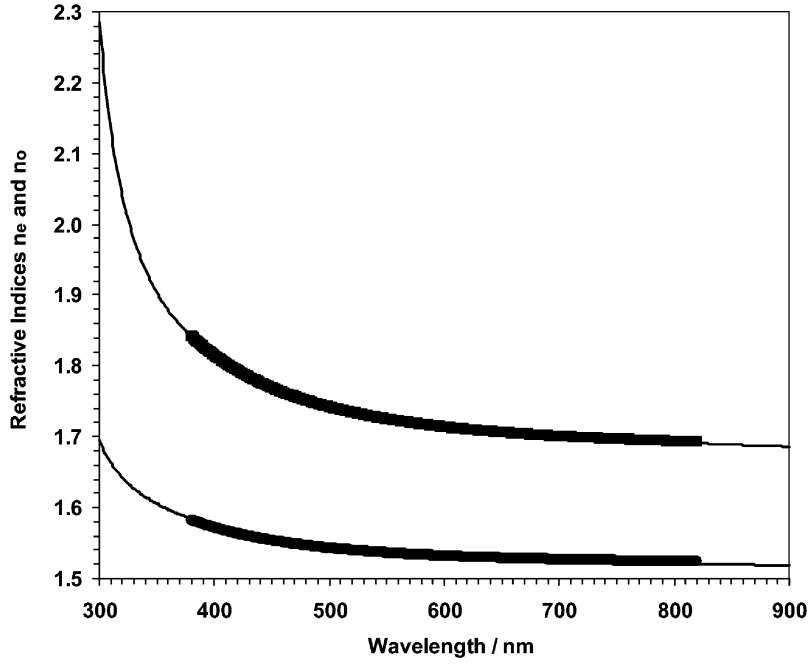

Figure 1. Calculated dispersion curves for the refractive indices of 5CB using the present model fitted to data from [9] with the fitting parameters given in tables 1 and 2 and $L_e=4\pi/3.7$, $S\approx0.61629$.

~0.8–0.87 obtained by Kedzierski *et al.* [25]. Since Kedzierski *et al.* found that the GFT anisotropy $\Delta L=L_o-L_e$ is linear with the order parameter S, it is possible that the averaging equations (18) and (19) apply also to L_o, L_e; however we shall show now that this issue is questionable. Using the value of the order parameter and assuming the averaging process of equations (18) and (19) applies, we get $L_\parallel\approx1.7542\pi$ and $L_\perp\approx2.3681\pi$. Using these latest values we find that 5CB is an oblate spheroid with a semi-axis ratio of $\rho\approx0.65$; or if we consider it as a cylinder then this corresponds to a radius to length ratio of $d/l\approx1.47$ (see the appendix). This does not seem realistic because these LCs are known to be positive uniaxial, therefore we raise the question whether the averaging process of equations (18) and (19) applies also to the GFT. In fact the ratio of $L_e/L_o\approx0.8$–0.87 obtained by Kedzierski *et al.* gives values of $L_\parallel$, $L_\perp$ even more unrealistic, and in particular that the molecules they studied have a larger length to width ratio. Without the averaging process (that is, using $L_{e,o}$ rather than $L_{\parallel,\perp}$), 5CB is found to be a prolate spheroid with $\rho\approx1.25$ or a cylinder with $l/d\approx1.07$, which is more realistic. The question whether the averaging process of equations (18) and (19) applies also to L_o, L_e remains to be clarified, perhaps with additional experimental data.

The strong effect of the GFT on the fit is demonstrated in figure 2 where the dispersion curves calculated for different values of L_e vary by up to 10%, demonstrating that it is very critical to know this parameter. A similarly strong effect, as expected, on the absorption spectra is shown in figure 3. Before performing the fit to the refractive indices we calculated the UV optical density spectra following the spectra presented by Wu [7], so that the same resonance wavelengths are obtained, the same spectral widths and peak heights. After this step we readily get the fit to the refractive indices shown in figure 1. Hence the measurement of the UV absorption spectra is a critical step towards a better understanding of the dispersion curves and the role of the anisotropic depolarization field.

By measuring the UV absorption spectra and making a fit using the present model to find the GFT, the calculation of the dispersion curves becomes more reliable. In particular, measurement of the UV absorption spectra as a function of temperature will indicate the temperature behaviour of the GFT. Measurements of the refractive indices and birefringence in the UV, for example down to 300 nm, will give added confidence for the damping factors. As seen in figure 4, the damping has little effect on the dispersion for wavelengths above 400 nm, and so generally the damping values used might not be accurate enough. However in this particular case we first made the fit to the absorption spectra and ensured that the extinction coefficient in the near infrared region is on the order of 0.001, close to the well known value. A note should be added here on the use of the Cauchy expansions. As shown in figure 5 the

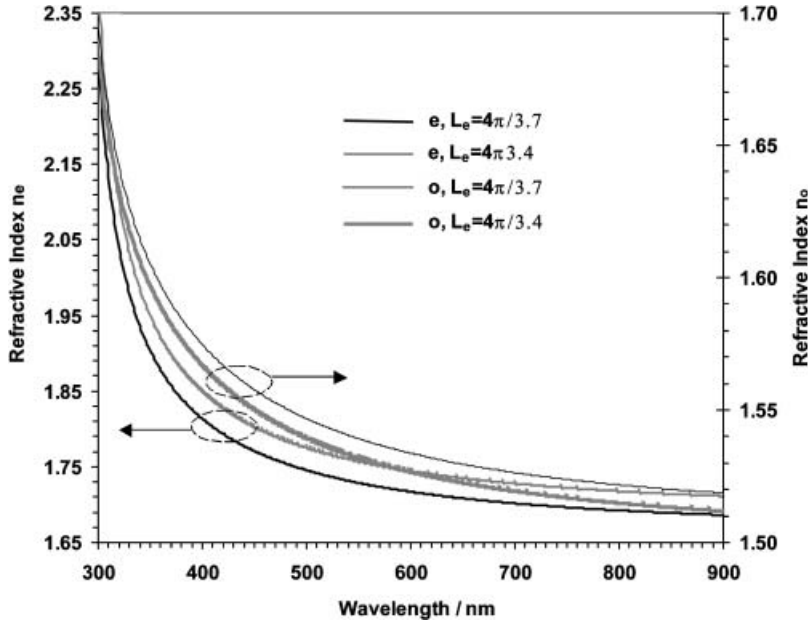

Figure 2. Calculated dispersion curves using the same parameters as used in figure 1 but for two different values of L_e, showing that it has a strong effect.

series expansion for the case of no damping up to the 5th order in the polarizability, equation (35), although it is excellent in the case of n_o, does not coincide completely with the exact curve in the case of n_e. Lower order expansions are unsatisfactory in both cases. Since the 5th order expansion in the polarizability can be converted into a 10th order expansion in the inverse wavelength, we can conclude that for the Cauchy expansion to be physically correct, a larger number of terms must be included in the expansion.

In order to gain additional confidence in the fitting parameters used for 5CB we compared our results with recent data obtained by Tkachenko *et al*. [36] using spectroscopic ellipsometry in the range 400–1700 nm.

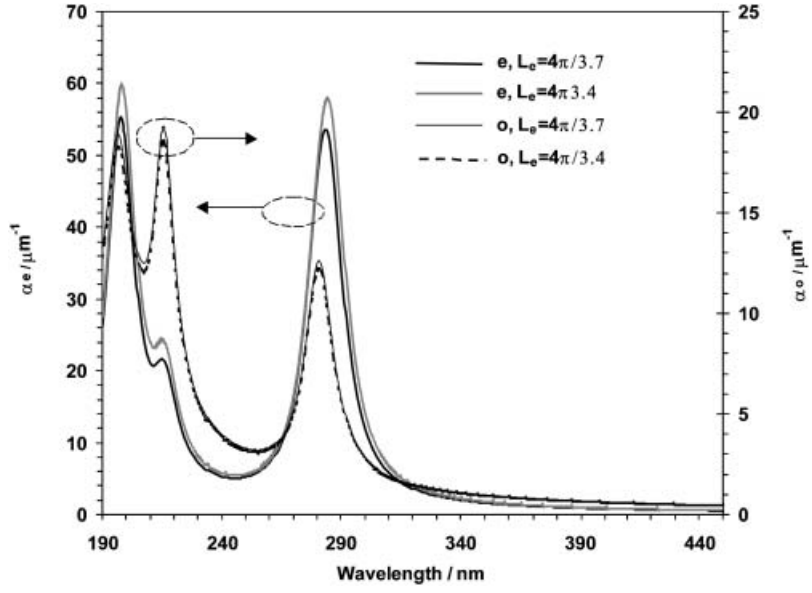

Figure 3. Absorption coefficients of 5CB calculated using the parameters used in figure 1 for two different values of L_e showing its strong effect. The absorption coefficient curves for $L_e=4\pi/3.7$ agree very well with the optical density measured in [7] using polarizing spectroscopy.

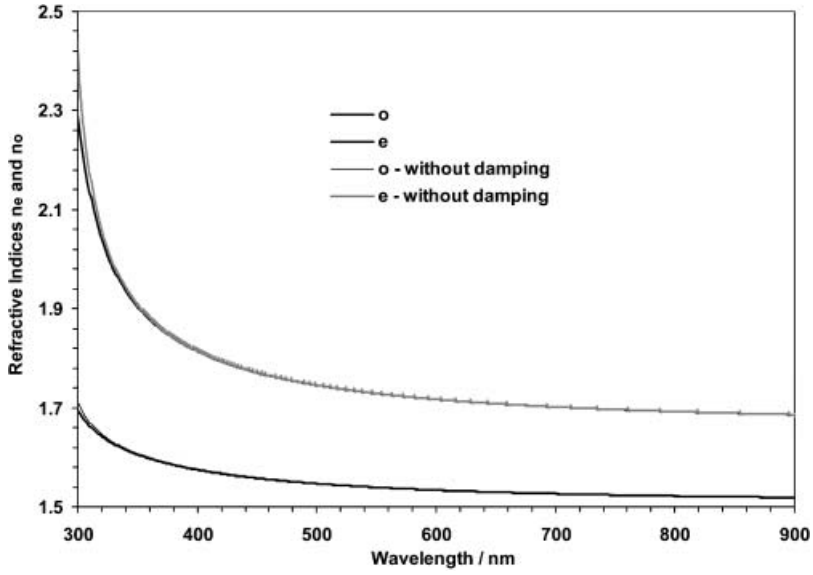

Figure 4. Effect of damping on the dispersion curves using the parameters of figure 1, showing that damping can affect the fit in the short wavelength region.

The comparison is shown in figures 6 and 7 where the only parameter changed is the order parameter calculated from $S=[(T_c-T)/T_c]^{0.142}$ with $T_c-T=5\,\mathrm{K}$. Their data is taken based on their Cauchy fit called Fit 2, which they found to be close to the fit of the data of Karat and Madhusudana [37]. The birefringence data (figure 7) were found based on their [36] Muller matrix fit (called MM Fit) to the spectroscopic ellipsometry data. The maximum difference between the measured and calculated values is smaller than 0.003 in the case of the birefringence, which is within their experimental accuracy as the temperature is accurate within $\pm 1\,\mathrm{K}$, leading to an inaccuracy of ± 0.005 in the birefringence. Perhaps to minimize the effect of temperature fluctuations one should measure at a temperature far from the transition temperature.

Another LC material that has been widely studied is the Merck material E7, which exhibits different resonance wavelengths. For comparison with experiment we took the data from [10] and used a fit on the

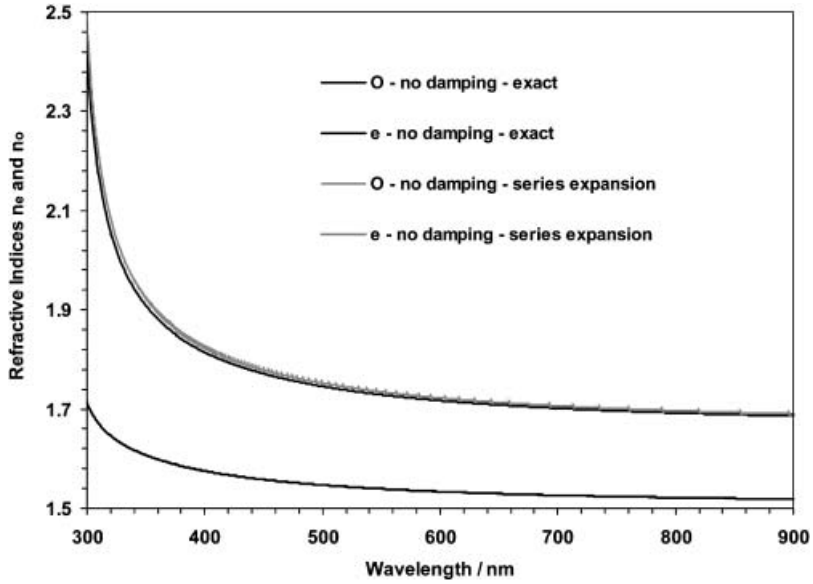

Figure 5. Comparison between exact dispersion curves and those obtained using the series expansion of equation (35) for the case of no damping, and using the same parameters of figure 1.

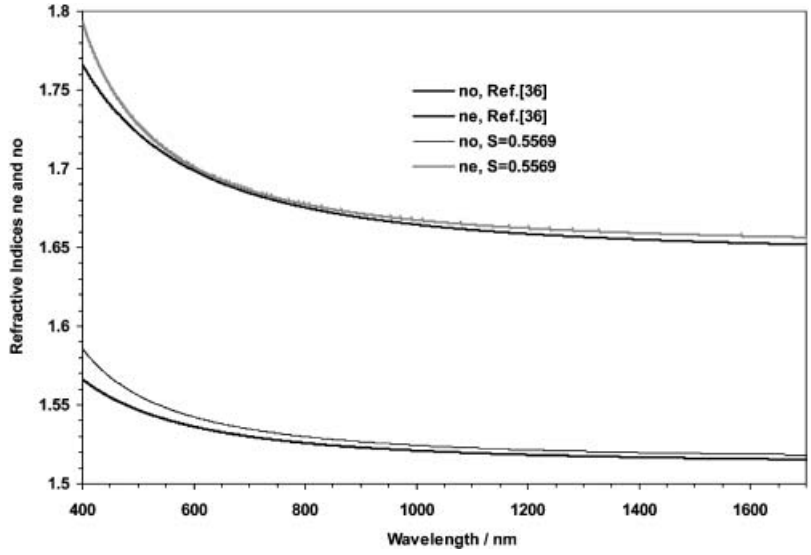

Figure 6. Comparison between dispersion curves of 5CB as measured in [36] and those obtained using the parameters of figure 1 but with a different order parameter $S \approx 0.5569$. The data of [36] were found from their Cauchy fit 2: $n_o = 1.5124 + 8600/\lambda^2$; $n_e = 1.6452 + 19300/\lambda^2$.

parameters listed in table 1 together with L_o, L_e, see figure 8. The calculated absorption spectra are shown in figure 9 where three bands are considered in this case leading to a satisfactory fit to the experimental data of the refractive indices (figure 8). The birefringence experimental data taken from two different sources as shown in figure 10 are remote from each other, while our calculated curves are somewhere between the two data sets. Additional experimental data for the birefringence is required to confirm the calculations.

6. Dispersion curve measurement using spectral retardation

The spectral retardation technique consists of measuring the retardation from the liquid crystal sample over a wide spectral range and performing the fit between the

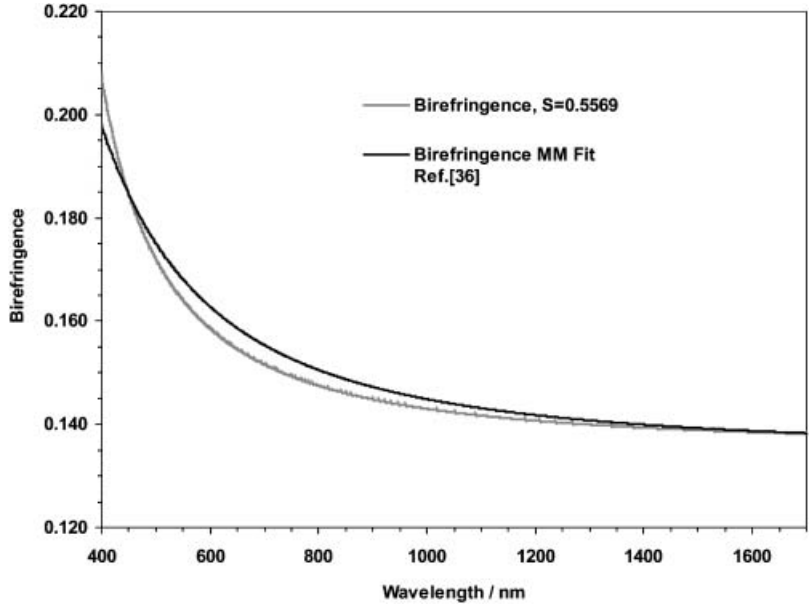

Figure 7. Comparison between measured birefringence dispersion curves of 5CB [36] and those obtained using the parameters of figure 1 but with the different order parameter $S \approx 0.5569$. The data of [36] were found from their Muller matrix fit: $\Delta n = 0.1348 + 10070/\lambda^2$.

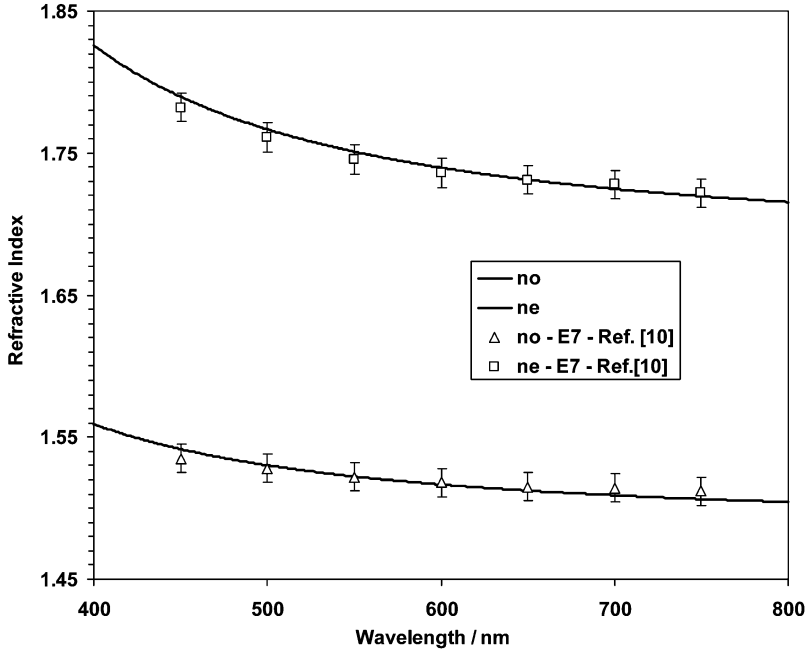

Figure 8. Calculated dispersion curves for the refractive indices of E7 using the present model fitted to the data of [10], with the fitting parameters given in tables 1 and 2 and $L_e=4\pi/3.2$, $S\approx0.72079$.

measured and calculated spectra with the refractive indices n_o, n_e as the fitting parameters. A small spot ($\sim$0.5 mm diameter) of polarized white light is incident on the sample, transmitted through it, then reflected using a mirror to return it back through the sample and then through a crossed polarizer. Figure 11 shows schematically the experimental set-up, where to maximize the contrast of the retardation peaks, the sample is oriented azimuthally such that the optic axis makes an angle of $\phi=45^\circ$ with the polarizer axis. The reflected light spectrum is analysed using a fibre-optic spectrometer with 1 nm resolution within the spectral range 400–850 nm. This configuration has two main advantages: (1) reflection-mode configuration is

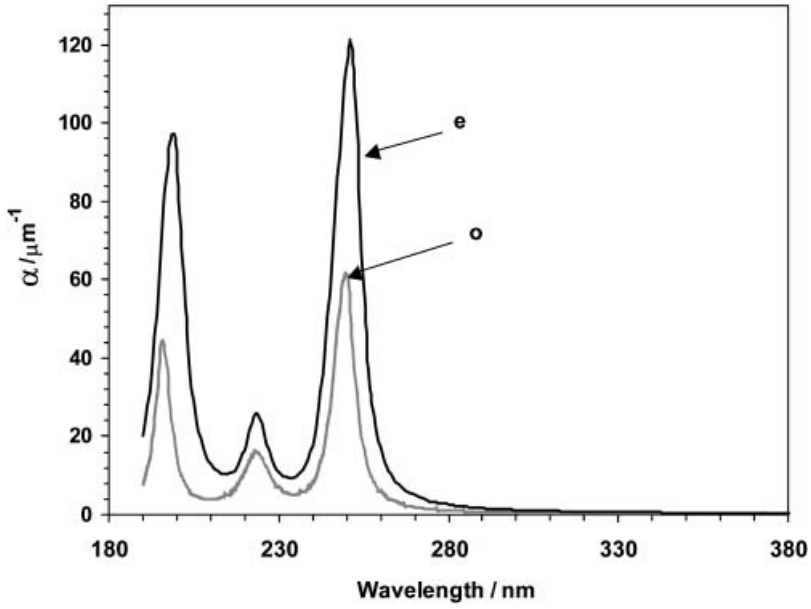

Figure 9. Absorption coefficients of E7 calculated using the parameters used in figure 8.

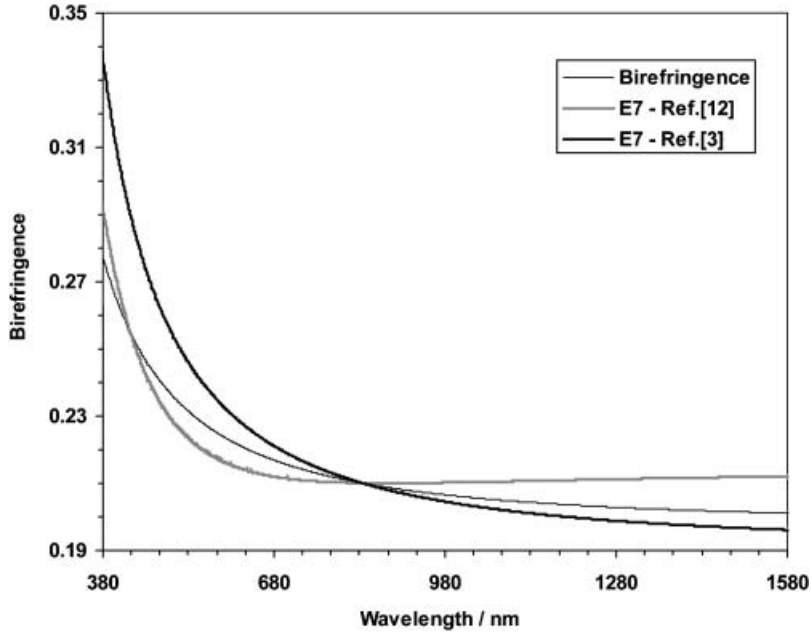

Figure 10. Comparison between measured birefringence dispersion curves of E7 from [3] and [12], and those obtained using the parameters of figure 8. The data of [3] found from their single band fit using $G=3.06\times10^{-6}\,\mathrm{nm}^2$, $\lambda^*=250\,\mathrm{nm}$. The data of [12] were found from the fit: $\Delta n=0.21437-6693/\lambda^2+2.591\times10^9/\lambda^4$.

preferable because it doubles the number of retardation peaks, thus the information content of the spectrum is larger; (2) the crossed-polarizers configuration minimizes the effect of reflections from the substrate boundaries. Further to minimize the effect of reflections from the boundaries, we took the reference signal as the average between the two spectra at the sample azimuth

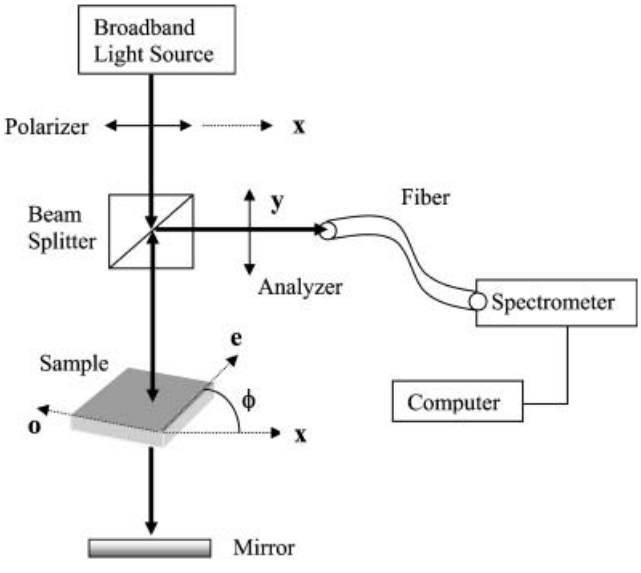

Figure 11. Schematic of the experimental set-up used for the refractive indices dispersion measurements of E44.

orientations $\phi=0^\circ$ and $\phi=90^\circ$ (the e and o orientations respectively) with the polarizers being parallel. The sample consisted of the LC material E44 homogeneously aligned between two glass plates using mechanical rubbing of a 20 nm thick HD2555 polyimide layer that is known to give a very small pretilt angle. The sample thickness was 15 μm achieved using Mylar spacers and confirmed using the fringe counting technique on the spectrum of an empty cell, measured using the same set-up but in a parallel polarizers configuration. Figure 12 shows the experimental data together with the calculation based on the transfer function of a retardation plate: $R=\sin^2[2\pi d(n_e-n_o)/\lambda]$ where the fitting parameters are n_o, n_e as a function of the wavelength. We found that the data similarly fit the exact calculations based on the analytic 4×4 matrix approach [38], because the glass substrates are anti-reflection coated and multiple reflections do not play a role. The dispersion curves measured based on this technique together with the calculated curves are shown in figure 13, exhibiting excellent agreement. The calculated curves are based on the three-bands absorption model as shown in figure 14 and using the parameters listed in table 1. We have also included one additional estimated point at 1550 nm, based on interferometric measurements at this particular wavelength.

To summarize, using the anisotropic Lorentz model for an oscillating dipole combined with the generalized Lorentz–Lorentz relationship, a dispersion relationship

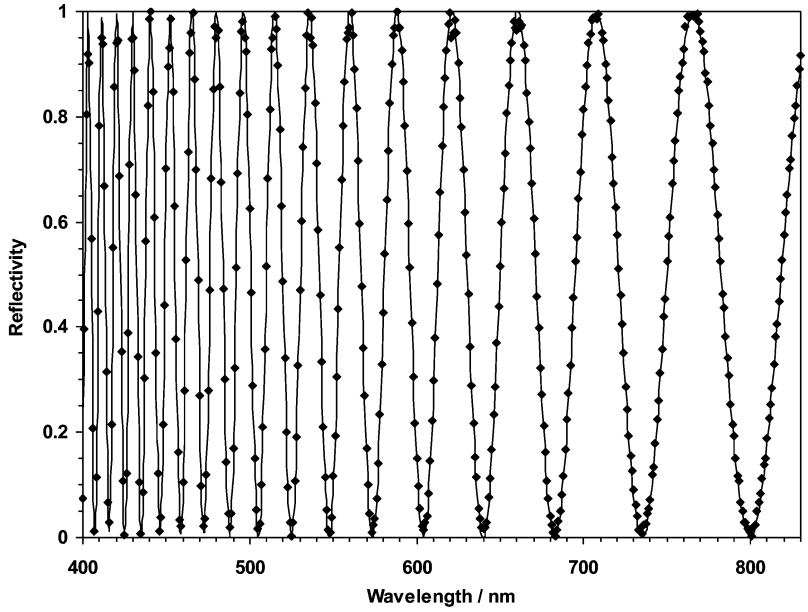

Figure 12. Measured and fitted reflectivity spectra using the spectroscopic retardation set-up described in figure 11 and in the text, on a 15 μm homogeneously aligned E44 LC cell in reflection mode.

is derived for the polarizability with the existence of damping. Based on this, a dispersion relationship for the refractive indices and absorption coefficients is derived and applied to liquid crystals. These relationships are consistent with the limiting cases of isotropic medium and spherical molecules, as well as with the well known dispersion formulae far from the absorption resonance when the medium becomes highly transparent and Sellmeier-type relationships apply. Comparison with experimental data shows good agreement when damping is taken into account, in particular for wavelengths in the visible range below 500 nm. Comparison with available

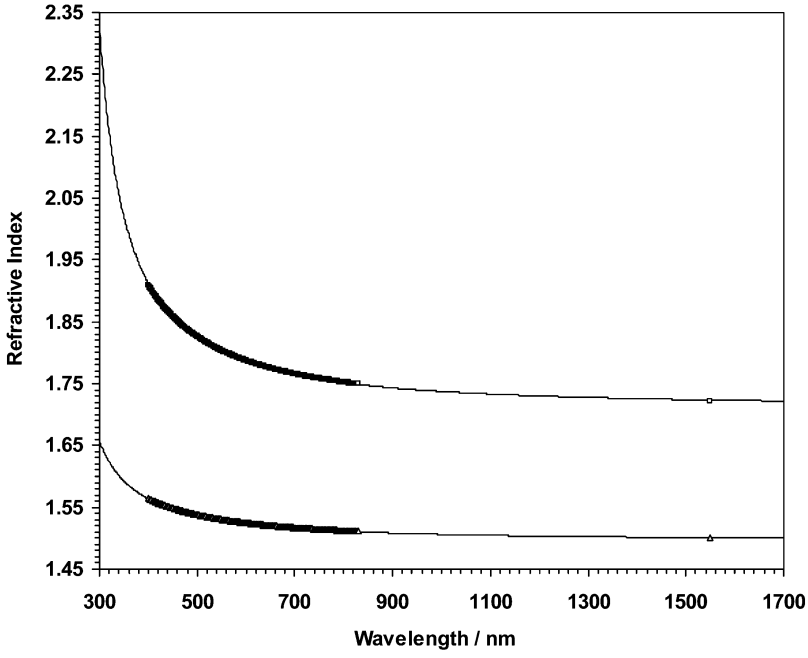

Figure 13. Measured and fitted refractive indices dispersion of E44 LC. The measured data are found from the fit between the calculated and measured reflectivity spectra shown in figure 12. The calculated curves were obtained using the present model with the parameters given in tables 1 and 2 and using $L_e=4\pi/3.15$, $S\approx 0.80044$.

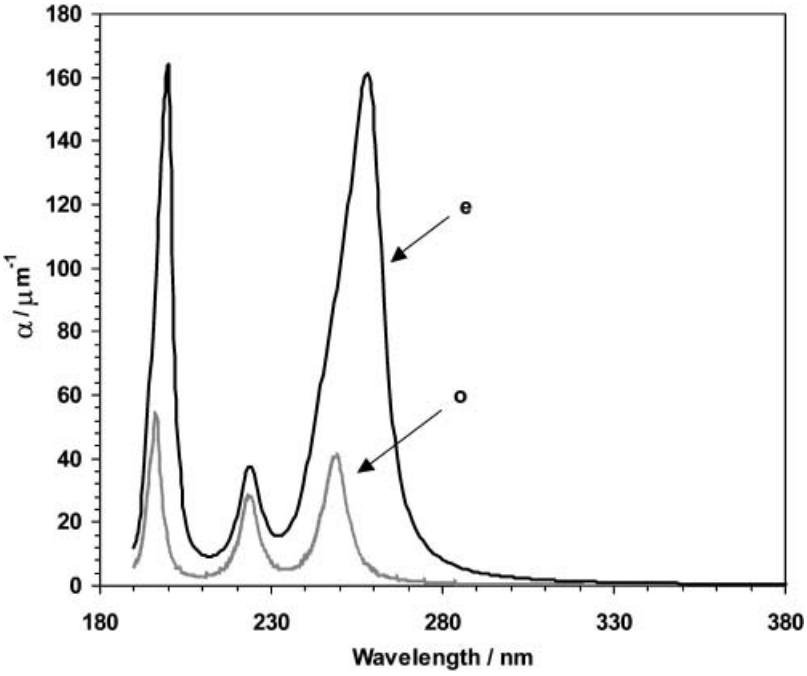

Figure 14. Absorption coefficients of E44 calculated using the parameters used in figure 13.

experimental data on several LC materials is presented and a measurement technique is described. From the measured spectral retardation on E44 LC the dispersion curves are found and compared with the model showing an excellent fit. The reflection mode spectral retardation technique has the advantages of doubling the path length and minimizing reflections from substrates using a crossed polarizers configuration and normalization to signals containing multiple reflections of the e and o waves. The expressions derived in this work and the spectral retardation technique are also useful for other ordered systems of molecules, such as rubbed or UV-oriented polymer or polyimide thin films used as alignment layers for liquid crystals [39]. Although these layers are usually thin, in the range of tens of nm, it is possible to enhance the signal-to-noise ratio by making them thicker or by modulating the light beam polarization in a similar manner to ellipsometry, or alternatively by performing phase-locked measurement.

Acknowledgement

Part of the experimental work was performed while the author was with GWS-Photonics Corporation.

References

[1] I.C. Khoo, S.T. Wu. *Optics and Nonlinear Optics of Liquid Crystals*. World Scientific, Singapore (1993).
[2] H. Mada, S. Kobayashi. *Mol. Cryst. liq. Cryst.*, **33**, 47 (1976).
[3] S.T. Wu. *Phys. Rev. A*, **33**, 1270 (1986).
[4] L. Lam, Z.C. Ou-Yang, M. Lax. *Phys. Rev. A*, **37**, 3469 (1988).
[5] S.T. Wu, C.S. Wu. *J. appl. Phys.*, **66**, 5297 (1989).
[6] I. Abdulhalim. *Mol. Cryst. liq. Cryst.*, **197**, 103 (1991).
[7] S.T. Wu. *J. appl. Phys.*, **69**, 2080 (1991).
[8] E.M. Averyanov. *J. opt. Technol.*, **64**, 417 (1997).
[9] J. Li, S.T. Wu. *J. appl. Phys.*, **95**, 896 (2004).
[10] M. Warenghem, C.P. Grover. *Rev. Phys. appl.*, **23**, 1169 (1988).
[11] M. Kawaida, T. Yamaguchi, T. Akahane. *Jpn. J. appl. Phys.*, **28**, L1609 (1989).
[12] O. Koysal, S.E. San, S. Ozder, F.N. Ecevit. *Meas. Sci. Technol.*, **14**, 790 (2003).
[13] C.J.F. Bottcher. *Theory of Electric Polarization,* 2nd Edn, Vol. I. Elsevier (1973).
[14] H.E.J. Neugebauer. *Can. J. Phys.*, **32**, 1 (1954).
[15] M.F. Vuks. *Opt. Spectrosk.*, **20**, 644 (1966).
[16] A. Saupe, W. Maier. *Z. Naturforsch*, **16a**, 816 (1961).
[17] S. Chandrasekhar, N. Madhusudana. *J. de Physique*, **30**, Colloq. C-4, 24 (1969).
[18] G. Pelzl. PhD thesis, University M. Lutter, Halle Germany (1969).
[19] W.H. de Jeu, W.A.P. Claassen. *J. chem. Phys.*, **68**, 102 (1978).
[20] W.H. de Jeu, P. Bordewijk. *J. chem. Phys.*, **68**, 109 (1978).
[21] I.H. Ibrahim, W. Haase. *Mol. Cryst. liq. Cryst.*, **66**, 189 (1981).
[22] N.V.S. Rao, V.G.K.M. Pisipati, P.V. Datta Prasad, P.R. Alapati, D. Saran. *Mol. Cryst. liq. Cryst.*, **132**, 1 (1986).
[23] P. Adamski. *Mol. Cryst. liq. Cryst.*, **177**, 1 (1989).
[24] P. Adamski. *Cryst. Res. Technol.*, **34**, 763 (1999).
[25] J. Kedzierski, Z. Raszewski, J. Rutkowska, W. Piecek, P. Perkowski, J. Zmija, R. Dabrowski, J.W. Baran. *Mol. Cryst. liq. Cryst.*, **282**, 205 (1996).

[26] I. Abdulhalim, G. Moddel. *Mol. Cryst. liq. Cryst.*, **200**, 79 (1991).
[27] I. Abdulhalim, G. Moddel, N.A. Clark. *Appl. Phys. Lett.*, **60**, 551 (1992).
[28] I. Abdulhalim, G. Moddel, N.A. Clark. *J. appl. Phys.*, **76**, 820 (1994).
[29] W. Maier, A. Saupe. *Z. Naturforsch.*, **15a**, 287 (1960).
[30] J.A. Osborn. *Phys. Rev.*, **67**, 351 (1945).
[31] E.C. Stoner. *Philos. Mag.*, **36**, 803 (1945).
[32] W.L. Bragg, A.B. Pippard. *Acta Cryst.*, **6**, 865 (1953).
[33] V. Twersky. *J. opt. Soc. Am.*, **65**, 239 (1975).
[34] B. Tatian. *Appl. Opt.*, **23**, 4477 (1984).
[35] J. Li, S. Gauza, S.T. Wu. *J. appl. Phys.*, **96**, 19 (2004).
[36] V. Tkachenko, A. Marino, F. Vita, F. D'Amore, L. De Stefano, M. Malinconico, M. Rippa, G. Abbate. *Electronic-Liquid Crystal Communications,* http://WWW.e-lc.org/docs/2004_02_26_11_59_53.
[37] P.P. Karat, N.V. Madhusudana. *Mol. Cryst. liq. Cryst.*, **36**, 51 (1976).
[38] I. Abdulhalim. *J. Opt. A*, **1**, 646 (1999).
[39] N.A.J.M. van Aerle, A.J.W. Tol. *Macromolecules*, **27**, 6520 (1994).
[40] E.M. Averyanov, V.F. Shabanov. *Kristallografiya*, **23**, 320 (1977).
[41] E.M. Averyanov, M.A. Osipov. *Usp. Fiz. Nauk*, **160**, 89 (1990).
[42] E.M. Averyanov. *Effekty lokalnowo pola w optikie zhidkikh kristallow,* Chaps. 2 and 3 (in Russian). Nauka, Nowosibirsk (1999).

Appendix

Expressions for the principal values of the depolarization form tensor

For an ellipsoid of uniform density with semi-axes a, b, c, the principal values of the form factor are given by the general integral [26, 27, 29, 40–42]:

$$L_q = 2\pi abc \int_0^\infty \frac{\mathrm{d}s}{\left(x_q^2+s\right)[(a^2+s)(b^2+s)(c^2+s)]^{\frac{1}{2}}} \quad \text{(A1)}$$

where $q=1, 2, 3$ and $x_1=a$, $x_2=b$, $x_3=c$. Normalization requires that $\sum_q L_q = 4\pi$. This general form of L_q for the biaxial case can be expressed in terms of elliptic integrals. For the uniaxial case the ellipsoid becomes an ellipsoid of revolution and the integral above is simplified. Assuming (a) the polar semi-axis and (b) the equatorial semi-axis, and defining the eccentricity $e=\left(1-\rho^2\right)^{\frac{1}{2}}$ where $\rho=a/b$, the following results are obtained. For a prolate spheroid ($\rho>1$):

$$L_a = \frac{4\pi\left(1-e^2\right)}{e^2}\left\{\frac{1}{2e}\ln\frac{1+e}{1-e}-1\right\}. \quad \text{(A2)}$$

For an oblate spheroid ($\rho<1$):

$$L_a = \frac{4\pi}{1-\rho^2}\left[1-\frac{\rho}{(1-\rho^2)^{\frac{1}{2}}}ar\cos\rho\right]. \quad \text{(A3)}$$

For a cylinder of diameter d and length l, the principal value along the cylinder axis is:

$$L_a = 4\pi\left[1-\frac{l}{(d^2+l^2)^{\frac{1}{2}}}\right]. \quad \text{(A4)}$$

In all cases (A2)–(A4) the principal values along the b-axis are found from the normalization condition:

$$L_b = \frac{1}{2}(4\pi - L_a). \quad \text{(A5)}$$